Published in final edited form as:
J Cell Sci. 2004 December 15; 117(Pt 26): 6473–6483. doi:10.1242/jcs.01580.

Role of myosin VIIa and Rab27a in the motility and localization of RPE melanosomes

Daniel Gibbs[1], **Sassan M. Azarian**[1], **Concepcion Lillo**[1], **Junko Kitamoto**[1], **Adriana E. Klomp**[1], **Karen P. Steel**[2,*], **Richard T. Libby**[2,‡], and **David S. Williams**[1,§]

[1]Departments of Pharmacology and Neurosciences, UCSD School of Medicine, La Jolla, CA 92093-0912, USA

[2]MRC Institute of Hearing Research, University Park, Nottingham, NG7 2RD, UK

Summary

Myosin VIIa functions in the outer retina, and loss of this function causes human blindness in Usher syndrome type 1B (USH1B). In mice with mutant *Myo7a*, melanosomes in the retinal pigmented epithelium (RPE) are distributed abnormally. In this investigation we detected many proteins in RPE cells that could potentially participate in melanosome transport, but of those tested, only myosin VIIa and Rab27a were found to be required for normal distribution. Two other expressed proteins, melanophilin and myosin Va, both of which are required for normal melanosome distribution in melanocytes, were not required in RPE, despite the association of myosin Va with the RPE melanosome fraction. Both myosin VIIa and myosin Va were immunodetected broadly in sections of the RPE, overlapping with a region of apical filamentous actin. Some 70–80% of the myosin VIIa in RPE cells was detected on melanosome membranes by both subcellular fractionation of RPE cells and quantitative immunoelectron microscopy, consistent with a role for myosin VIIa in melanosome motility. Time-lapse microscopy of melanosomes in primary cultures of mouse RPE cells demonstrated that the melanosomes move in a saltatory manner, interrupting slow movements with short bursts of rapid movement (>1 μm/second). In RPE cells from *Myo7a*-null mice, both the slow and rapid movements still occurred, except that more melanosomes underwent rapid movements, and each movement extended approximately five times longer (and further). Hence, our studies demonstrate the presence of many potential effectors of melanosome motility and localization in the RPE, with a specific requirement for Rab27a and myosin VIIa, which function by transporting and constraining melanosomes within a region of filamentous actin. The presence of two distinct melanosome velocities in both control and *Myo7a*-null RPE cells suggests the involvement of at least two motors other than myosin VIIa in melanosome motility, most probably, a microtubule motor and myosin Va.

Keywords

Myosin VIIa; Myosin Va; Rab27a; Melanosome; Usher syndrome; Organelle motility

§Author for correspondence (dswilliams@ucsd.edu).
*Present address: Wellcome Trust Sanger Institute, Hinxton, Cambridge, CB10 1SA, UK
‡Present address: The Jackson Laboratory, 600 Main Street, Bar Harbor, ME 04609, USA

Supplementary material available online at http://jcs.biologists.org/cgi/content/full/117/26/6473/DC1

Introduction

Mutations in any one of seven different genes can effect the same type of deafness-blindness that is characterized by Usher syndrome type 1 (USH1) (Petit, 2001; Mustapha et al., 2002). Thus, there are seven subtypes of USH1, USH1A through USH1G. USH1B accounts for at least half of USH1 cases (Astuto et al., 2000). It is caused by mutations in *MYO7A*, which encodes the unconventional myosin, myosin VIIa (Weil et al., 1995). Shaker1 mice have mutations in the orthologous gene (Gibson et al., 1995). Although these mice do not undergo retinal degeneration, several mutant phenotypes are evident in their retinas (Liu et al., 1998; Liu et al., 1999; Libby and Steel, 2001; Gibbs et al., 2003). One of these is an aberrant distribution of the melanosomes in the RPE. Melanosomes are absent from the apical region of mutant RPE in original shaker1 mice ($Myo7a^{sh1}$) (Liu et al., 1998).

Melanosome transport and localization has been best studied in the amphibian melanophores and in mammalian melanocytes. In the latter, melanosomes are localized in the periphery by a protein complex that links the melanosome to the actin cytoskeleton. Rab27a on the melanosome membrane binds melanophilin (Slac2-a), which in turn binds the actin-based motor, myosin Va (Fukuda et al., 2002; Nagashima et al., 2002; Strom et al., 2002; Wu et al., 2002). Loss of myosin Va, Rab27a, or melanophilin results in dilute phenotypes in mice and humans (Mercer et al., 1991; Pastural et al., 1997; Wu et al., 1998a; Wilson et al., 2000; Menasche et al., 2000; Wu et al., 2001; Hume et al., 2001; Matesic et al., 2001; Hume et al., 2002). Melanophilin is a Rab27 effector and a member of the exophilin family (Matesic et al., 2001). Myrip (or Slac2-c) is another Rab27 effector, and joins melanophilin and Slac2-b in the exophilin subgroup of those lacking C2 domains (Fukuda and Kuroda, 2002). Myrip has been immunodetected in RPE and shown to bind both myosin VIIa and Rab27a in vitro (El-Amraoui et al., 2002; Fukuda and Kuroda, 2002). Hence, it has been suggested that the complex, Rab27a-Myripmyosin VIIa, might localize RPE melanosomes along actin filaments just as Rab27a-melanophilin-myosin Va localizes melanosomes in the melanocytes (El-Amraoui et al., 2002). However, Myrip is present in many places where myosin VIIa is not, and, like melanophilin, can bind actin directly (without needing a myosin) (Fukuda and Kuroda, 2002; Desnos et al., 2003; Waselle et al., 2003), suggesting that the functions of these proteins are more complex than offering a simple tripartite parallel between melanocytes and RPE cells.

We have explored the molecular mechanisms underlying the distribution of RPE melanosomes, and have thus tested elements of the Rab27a-Myrip-myosin VIIa hypothesis. We show the presence of many different potential components of melanosome motility and localization in the RPE, suggesting the involvement of more than just these three proteins. Nevertheless, we found that correct melanosome localization specifically requires Rab27a and myosin VIIa, which function by transporting and constraining melanosomes within a region of filamentous actin.

Materials and Methods

Animals

The genetic backgrounds of the following alleles of shaker1 mice, $Myo7a^{816SB}$, $Myo7a^{26SB}$, $Myo7a^{3336SB}$, $Myo7a^{4494SB}$ and $Myo7a^{6J}$, were as described previously (Libby and Steel, 2001). $Myo7a^{4626SB}$ mice were backcrossed to mice of the C57BL/6 background. The $Myo7a^{sh1}$, $Myo7a^{7J}$ and $Myo7a^{8J}$ mice were bred directly from the animals received from The Jackson Laboratory (and thus maintained on the same genetic background). The $Myo7a^{9J}$ mice were backcrossed twice to mice of the CBA/Ca background and interbred for one to five generations. Snell's waltzer ($Myo6^{sv}$) mutants and waltzer 2J ($Cdh23^{v-2J}$) mutants, both on the C57BL/6J background, were obtained from The Jackson Laboratory. The shaker1, waltzer and Snell's waltzer stocks were maintained using homozygote by heterozygote matings to provide

both homozygous mutants and heterozygous littermate controls, which were distinguished by the head-bobbing and circling behavior of homozygotes associated with vestibular dysfunction.

A pair of Ames' waltzer 3J mice (*Pcdh15*$^{av\text{-}3J/av\text{-}3J}$) on a C57BL/6J background were obtained from The Jackson Laboratory and used directly for the present experiments.

Three dilute genotypes were bred and analyzed, *Myo5a*$^{d\text{-}l}$/*Myo5a*$^{d\text{-}l}$; *Myo5a*^{d}/*Myo5a*$^{d\text{-}l}$ and *Myo5a*^{d}/*Myo5a*^{d}, as described previously (Libby et al., 2004). The dilute lethal homozygotes were identified by progressive hind limb paralysis. They and their littermates were examined at 20–23 days of age before the health of these homozygotes was seriously affected. Dilute homozygotes and compound heterozygotes were distinguished by their pinna size, because the dilute allele was closely linked to the short ear mutation (*Bmp5*^{se}), such that dilute homozygotes had short ears and compound heterozygotes had normal length ears.

Control (*Rab27a*$^{+/ash}$) and mutant (*Rab27a*$^{ash/ash}$) ashen mice were obtained from a single litter, bred by the Mouse Mutant Resource at the Jackson Laboratory. The mice were on the C3H/HeSn background, which includes the *rd1* mutation. Retinas were obtained from 14-day-old animals. No photoreceptor outer segments are present in these retinas because of the initiation of photoreceptor degeneration, however, the RPE remains unaffected by degeneration at this stage.

Melanophilin mutant mice (*Mlph*, leaden mice) were obtained from the Mouse Mutant Resource at The Jackson Laboratory. The mice were on the DW/J background, and carried a mutation in *Pit1* (DW/J *Mlph*^{ln} *Pit1*^{dw}/*J*). All mutant mice were either wild type or heterozygous for *Pit1* (pit1 heterozygotes are phenotypically indistinguishable from wild type). Control mice were from a separate strain of mice (DW.C3-*Mlph*$^{+}$ *Pit1*$^{+}$/*J*). This strain was identical to the mutant strain used, except that the strain contains congenic regions for wild-type alleles of *Mlph* and *Pit1* (donated from strain C3H/HeJ). Mutant mice were 5–7 months old and control mice were 8 months old.

All mice, except the ashen and leaden mice (which were used directly from Jackson Laboratory stocks), were maintained on a 12 hour light/12 hour dark cycle, with exposure to 10–50 lux of fluorescent lighting during the light phase. They were treated according to UK Home Office, NIH and UCSD animal care guidelines.

Purification of RPE cells

RPE cells were prepared from mouse or pig eyes, following the procedure essentially as described previously (Wang et al., 1993). Pig eyes were obtained from a local abattoir. For further purification, the RPE sheets were laid on top of an 8%–15%–30% Optiprep (Greiner, FL, USA) step-gradient in CFHE buffer (5.4 mM KCl, 0.4 mM KH_2PO_4, 0.8 mM $MgSO_4$, 137 mM NaCl, 0.34 mM Na_2HPO_4, 2.0 mM EDTA, 0.03 mM Phenol Red, 5.5 mM D-glucose, 10 mM Hepes, pH 7.4), centrifuged for 20 minutes at 12,000 ***g***, and collected from the 15%–30% interface.

RT-PCR

Poly(A)$^{+}$ RNA was isolated from mouse RPE cells or tissue, using the Quickprep Micro mRNA purification kit (Amersham Biosciences, NJ, USA). For first-strand cDNA synthesis, mRNA was used as template, using Superscript II reverse transcriptase (Invitrogen, CA, USA) and oligo(dT) as primer. PCR was performed using specific primers as described in Table 1. All reactions were performed in the presence of positive and negative controls.

Subcellular fractionation of RPE cells

Purified pig RPE cells were suspended in 5 ml CFHE, including protease inhibitors, and snap-frozen in liquid nitrogen. The thawed suspension was passed 10 times through a 25-gauge needle. The lysate was centrifuged for 10 minutes at 60 ***g***, and 4°C, to pellet nuclei, unlysed cells, and other debris. The supernatant was kept on ice while the pellet was washed, and the supernatants were combined (S1). S1 was centrifuged again and the pellet was combined with the first one, as P1. S1 was centrifuged for 10 minutes at 2500 ***g*** and 4°C, to obtain the melanosome-enriched pellet, P2. P2 was resuspended in CFHE and laid on a 50% Optiprep/CFHE cushion for centrifugation at 12,000 ***g*** for 20 minutes at 4°C. By light microscopy, the resulting pellet (GP) consisted almost exclusively of melanosomes and was shown to be devoid of nuclei after staining with Trypan Blue. The interface (GI) and the rest (GR) of the gradient were also collected for analysis.

Antibodies

The myosin VIIa polyclonal antibody pAb2.2, was purified by affinity chromatography against the bacterially expressed antigen (Liu et al., 1997) coupled to an NHS-Sepharose column (Amersham, CA). Alternatively, pAb2.2 antiserum was purified by repeated depletion against western blots of retinal tissue from homozygous *Myo7a*^{4626SB} mice (which are null for *Myo7a*). Myosin Va polyclonal antibody DIL2, was used as provided by Dr John Hammer. It was made against a fusion protein corresponding to amino acids 910–1106 of human myosin Va, and does not appear to cross react with myosin Vb or Vc (Wu et al., 1997; Wu et al., 1998b). The HSP60 monoclonal antibody was obtained from Stressgen (Victoria, Canada).

Western blot analysis of RPE cell fractions

Aliquots of each fraction, originating from the equivalent of 25% of the RPE from one pig eye, were solubilized in Laemmli sample buffer and loaded on a 10% highly porous sodium dodecyl sulphate-polyacrylamide gel for electrophoresis (SDS-PAGE) (Doucet and Trifaro, 1988). Following electrophoresis the intact stacking gel was dried on a Whatman 3MM paper and photographed to show the distribution of melanosomes. (Melanin remains at the bottom of the wells and does not enter the stacking gel.) The running gel was transblotted on to immobilon-P and immunolabeled with myosin VIIa antibody and alkaline phosphatase-conjugated secondary antibody for staining with nitro blue tetrazolium chloride/5-bromo-4-chloro-3′-inodylphosphate p-toluidine salt (NBT/BCIP). After photography, the same blot was stripped for 15 minutes in 0.2 M glycine, pH 2.5, blocked, and immunolabeled with myosin Va antibody. The amount of antigen in each sample was quantified by densitometry against a twofold dilution series of the lysate as standards.

Light and electron microscopy

Purified RPE cells and retinas were fixed with 2% glutaraldehyde + 2% paraformaldehyde in 0.1 M cacodylate buffer, pH 7.4, and embedded in Epon 812. Retinas were fixed by either perfusion of the whole animal or immersion of the eyecup. Semithin sections (0.7 μm, stained with Toluidine Blue) and ultrathin sections were analyzed by light and electron microscopy, respectively.

For immunofluorescence microscopy, eyes were fixed in 4% paraformaldehyde in PBS. Eyecups were cryoprotected in 30% sucrose in PBS overnight at 4°C, and embedded in OCT compound (Ted Pella, CA, USA). Thick (8 μm) cryosections were collected on polylysine-coated glass slides. Autofluorescence was quenched with 0.1% sodium borohydride in phosphate-buffered saline (PBS). Sections were incubated with primary antibody overnight at 4°C in blocking solution (2% goat serum, 0.1% Triton X-100 in PBS), and secondary antibody for 1 hour at room temperature in the dark using the Alexa 594 nm or 488 nm goat anti-rabbit

IgG (Molecular Probes, OR, USA). Nuclei and F-actin were labeled with DAPI (diluted 1:10,000) and BODIPY FL or TR-X phallacidin (diluted 1:200), respectively (Molecular Probes, OR, USA). Sections were mounted using Mowiol mountant (Calbiochem, CA, USA). Images were collected with a BioRad 1024 laser scanning confocal microscope.

For immunoelectron microscopy, eyecups were fixed by immersion in 0.1% glutaraldehyde + 2% paraformaldehyde in 0.1 M cacodylate buffer, pH 7.4, and processed for embedment in LR White. Ultrathin sections were etched with saturated sodium periodate (Sigma, St. Louis, MO, USA), blocked with 4% bovine serum albumin (BSA) in Tris-buffered saline (TBS) for 1 hour, incubated with purified myosin VIIa antibody in TBS + 1% BSA + 1% Tween 20 overnight at 4°C, washed, incubated with goat anti-rabbit IgG conjugated to 10 nm gold (Amersham, Arlington Heights, IL, USA) in TBS + 1% BSA + 1% Tween 20 for 1 hour, postfixed with 2% glutaraldehyde for 20 minutes, washed, and stained with 2% ethanolic uranyl acetate for 15 minutes and lead citrate for 10 minutes. Negative control sections processed at the same time included labeled sections from *Myo7a*$^{4626SB/4626SB}$ retinas and sections from the same retinas that were incubated with 1 mg/ml of the original antigen fusion protein together with the myosin VIIa antibody.

Primary RPE cell culture

Primary RPE cells were isolated from 10- to 12-day-old *Myo7a*$^{+/4626SB}$ and *Myo7a*$^{4626SB/4626SB}$ littermates, as described previously (Gibbs et al., 2003; Gibbs and Williams, 2003). They were plated on to 35-mm plastic dishes and grown for 7 days in Dulbecco's modified Eagle's medium (DMEM), high glucose (Invitrogen, CA, USA), supplemented with 10% fetal bovine serum, 1% MEM non-essential amino acids (Invitrogen, CA, USA) and 1% penicillin-streptomycin (Invitrogen, CA, USA). Cells were grown on plastic rather than filters for clearer phase-contrast and bright-field microscopy.

Time-lapse microscopy of melanosome dynamics

Twenty-four hours prior to observation, primary RPE cells were cultured in fresh growth medium buffered with 10 mM Hepes and maintained in this medium for the duration of the experiments. The dynamics of motile melanosomes in living cells were visualized by time-lapse bright-field microscopy, using a 40× air objective on a Nikon inverted microscope. The temperature of the RPE cells was measured using a thermocouple placed into the growth medium and was maintained at 37°C±0.5°C using a hot air source. For each time course, the cells and microscope were equilibrated at 37°C for 30 minutes prior to observation. Lots of 700 images were captured at 500 millisecond intervals (i.e. total period of 350 seconds) with a Photometrics Quantix CCD camera (Roper Scientific, AZ, USA). Image acquisition was controlled using the Metamorph software (Universal Imaging Corp, PA, USA) running on a Dell Pentium computer.

Quantitative analysis of motile melanosomes

Metamorph image stacks of a time series were imported into the ImageJ software package (http://rsb.info.nih.gov/ij/). Kymographs measuring the displacement over time of motile melanosomes in primary RPE cells from *Myo7a*$^{+/4626SB}$ and *Myo7a*$^{4626SB/4626SB}$ mice were generated using the Multiple Kymograph plugin (http://www.embl-heidelberg.de/eamnet/html/body_kymograph.html), written by J. Rietdorf (rietdorf@embl.de). Displacement was determined only in two dimensions within the plane of focus of the objective. Displacement in the z-axis was relatively insignificant because the cells were relatively flat as a result of growth on plastic. The rare melanosome that did move excessively in the z-axis disappeared from the image plane and was thus disregarded. The velocity of moving objects is directly proportional to the gradient of the kymograph trace, and was measured by calculating the arc tangent from linear regions of the kymograph, representing

directed motion. A total of 107 motile melanosomes were sampled randomly from each of *Myo7a*$^{+/4626SB}$ and *Myo7a*$^{4626SB/4626SB}$ primary RPE cells from three separate cultures.

Results

Candidate components of melanosome transport in the RPE

The presence of candidate proteins was determined by RT-PCR and western blot analyses of purified RPE cells. Sheets of RPE were isolated from mouse or pig retinas, and then purified over Optiprep gradients. RPE cells purified in this manner were determined by light and electron microscopy to be essentially free of material from other cell types, including outer segment disk membranes from photoreceptor cells. The cells retained their polarity, with their apical processes forming a distinct region (Fig. 1). As Fig. 1 also shows, the difference in melanosome distribution and orientation between control and shaker1 RPE is maintained in these purified sheets.

RT-PCR was performed seven times from different preparations of purified sheets of RPE cells. Detection was determined to be positive if a signal was evident in at least five out of the seven trials. Thus, Rab27a, melanophilin, Myrip, myosin VIIa and myosin Va were detected in the RPE cells but Rab27b was not (Fig. 2A). In a comprehensive test for the presence of all known members of the exophilin (Rab27 effector) family, exophilins 1 (rabophilin 3a), 4 (Sytl2), 5 (Slac2-b), 6 (Sytl3) and 7 (Sytl1) were also detected, but exophilins 2 (granuphilin, Sytl4) and 9 (Sylt5) were not (Fig. 2B).

Requirement of proteins for normal melanosome distribution in RPE cells

The RT-PCR results indicated a broad range of potential participants in melanosome motility and localization. To determine whether or not a given protein was required for melanosome localization, we examined retinas of mice lacking that protein. These studies were limited by the availability of mutant mice, so that we were unable to test all RT-PCR positives; but we were able to include tests for some additional potential participants.

Previously, we had found that melanosomes were absent from the apical processes of RPE in the original *Myo7a* mutant (*Myo7a*^{sh1}) (Liu et al., 1998), which has a missense mutation (Gibson et al., 1995) and a level of mutant protein that is comparable to that of wild-type protein in controls (Hasson et al., 1997). We have now examined retinas from homozygous mutants of all ten known *Myo7a* alleles, as well as compound heterozygous *Myo7a*$^{4626SB/9J}$ mice. Melanosomes were similarly mislocalized in all cases. The outer retina of a *Myo7a*$^{4626SB/4626SB}$ mouse, which is an effective null mutant (Hasson et al., 1997; Liu et al., 1999), is shown together with that of a heterozygous control in Fig. 3A and B. In control retinas, some melanosomes have entered the apical processes with their long axis parallel to the apical processes (and the rod outer segments) (Fig. 3A). In the mutants, melanosomes are oriented more randomly and none are in the apical processes (Fig. 3B). This difference was detectable as early as 7 days post natum, when the photoreceptor cells are not fully developed, possessing only the first disk membranes of the outer segment, and the RPE apical membrane is not yet fully amplified (not shown). As noted above, this difference is also evident in isolated sheets of RPE cells (Fig. 1).

In vitro protein binding studies have shown linkage among different USH1 proteins, including myosin VIIa, by way of binding to the PDZ domains of harmonin, the USH1C protein (Boeda et al., 2002; Siemens et al., 2002; Weil et al., 2003). Of particular relevance to retinal function, double homozygous *Cdh23* (USH1D orthologue) and *Myo7a* mutant mice (~12 months of age) showed evidence of mild retinal degeneration, which was absent in mice that were homozygous mutant for either of the genes alone (Lillo et al., 2003). To test for an interaction between

myosin VIIa and other USH1 proteins with respect to RPE melanosome localization, we examined the retinas of available mice with mutations in USH1 orthologues. In contrast to the RPE melanosomes of *Myo7a*-mutant mice, those in mice homozygous for either the *Pcdh15*$^{av\text{-}3J}$ (Ames waltzer) or *Cdh23*$^{v\text{-}2J}$ (waltzer) mutant alleles were localized correctly (Fig. 3D,F). Even in homozygous mutant *Cdh23*$^{v\text{-}2J}$ mice that were also heterozygous for the *Myo7a*^{4626SB} mutation, melanosomes were localized normally in the RPE (Fig. 3I). Thus, we detected no requirement for either the USH1D (CDH23) or USH1F (PCDH15) protein in the localization of RPE melanosomes, and no indication of an interaction with myosin VIIa in this function.

Next, we tested whether other unconventional myosins might also participate in the localization of RPE melanosomes. It has been suggested that there might be some redundancy in retinal myosin function, which, in varying degrees, might account for the difference in susceptibility to retinal degeneration as a result of mutant myosin VIIa between man and mouse. Myosin Va is the most obvious candidate to function in RPE melanosome localization for, in addition to its participation in the localization of melanosomes in melanocytes, it was detected in the RPE and in association with RPE melanosomes (see below). Another candidate is myosin VI. Like myosin VIIa, myosin VI is required for normal hair cell function (Avraham et al., 1995; Ahmed et al., 2003; Melchionda et al., 2001). Moreover, mice that are homozygous mutant for myosin VI have compromised retinal physiology, as measured by electroretinograms (ERGs) (own unpublished observations), similar to mice lacking myosin VIIa (Libby and Steel, 2001) or myosin Va (Libby et al., 2004). Nevertheless, the distribution of RPE melanosomes was normal in mice homozygous for the *Myo5a*^{d} (dilute), *Myo5a*$^{d\text{-}l}$ (dilute lethal) or *Myo6*^{sv} (Snell's waltzer) mutations. Even in mice homozygous mutant for *Myo5a*$^{d\text{-}l}$ that were also heterozygous for *Myo7a*^{4626SB}, melanosomes were localized normally (Fig. 3G).

Last, we examined mice lacking Rab27a (*Rab27a*$^{ash/ash}$) or melanophilin (*Mlph*$^{ln/ln}$), both of which were detected in normal RPE (Fig. 2) (mice lacking Myrip were not available). In *Rab27a*$^{ash/ash}$ mice, the RPE melanosomes were mislocalized, just like those of *Myo7a*-mutant mice. They were absent from the apical region and oriented more obliquely with respect to the direction of incoming light (Fig. 4) (Futter et al., 2004). However, melanosomes were distributed normally in the RPE of *Mlph*$^{ln/ln}$ mice (Fig. 3J).

None of the mutations examined appeared to affect the number or size of melanosomes. This observation was confirmed quantitatively for *Mlph*$^{ln/ln}$ mice, which had a mean of 8551 melanosomes in each complete dorsoventral section (n=2), compared with a mean of 8877 in controls (n=2).

Association of myosin VIIa and myosin Va with RPE melanosomes

The presence of myosin VIIa in the apical RPE has been reported previously (Hasson et al., 1995; El-Amraoui et al., 1996; Liu et al., 1997). Myosin Va is more broadly distributed in the retina, with a particularly high concentration in the photoreceptor synapses (Schlamp and Williams, 1996), where it is required for normal function (Libby et al., 2004). Here, we have immunolabeled both myosins in the RPE of serially sectioned mouse retinas and compared their distribution with that of actin filaments, using confocal microscopy. Myosin VIIa occupies an area of the RPE that extends from the cell nuclei to a region overlapping the apical network of actin filaments; it does not, however, extend all the way down the apical processes (Fig. 5A). Myosin Va was found to be similarly distributed in the RPE, with a similar region of overlap with actin filaments (Fig. 5B).

Subcellular fractionation of purified sheets of pig RPE cells was performed to test for association of these two myosins with melanosomes. In the procedure outlined in Fig. 5C, melanosomes from lysed cells were collected in S1, and then sedimented in P2. When the

contents of P2 were layered on top of 50% Optiprep and centrifuged, remaining intact cells did not enter the Optiprep, while essentially pure melanosomes collected at the bottom of the tube. Western blots labeled with myosin VIIa and myosin Va antibodies showed that both myosins were distributed similarly among the different fractions (Fig. 5C). From densitometric scans of the western blots, we determined that 85% of myosin VIIa and myosin Va from S1 was collected in P2. Of that fraction, most was associated with the melanosomes following centrifugation through the 50% Optiprep. Our data from different experiments indicate that ~80% of the myosin VIIa, and a similar percentage of myosin Va, is associated with RPE melanosomes. This association appears to be with the melanosomes membrane, and not with melanin that might be exposed by rupture of the melanosomes membrane. Both myosins became readily soluble after washing the melanosomes with buffered 1% SDS.

In the first published image of immunoelectron microscopic localization of myosin VIIa in the RPE, myosin VIIa was shown to be in the apical cytoplasm of human RPE, unassociated with the melanosomes (Liu et al., 1997). Subsequently, immunolabel was shown on melanosomes in a small, high magnification image from mouse RPE (El-Amraoui et al., 2002). Neither of these studies presented any quantification of label or any further data on RPE localization of myosin VIIa beyond their single image. Our fractionation experiments indicate that, in pig RPE, much (80%) of the myosin VIIa is associated with the melanosomes and some (20%) is not (Fig. 5C). This observation is supported by quantitative immunoelectron microscopy of mouse retinas. We counted the number of gold particles within 30 nm of the melanosome membrane (approximately the maximal distance a gold particle could be located from the antigen, given the size of two IgG molecules) and elsewhere in the RPE cytoplasm (circles and arrows, respectively, in Fig. 6). As illustrated in Fig. 7A, a mean of 75% of the myosin VIIa label was associated with melanosome membranes. We also divided the RPE into two regions, apical or basal to the adherens junctions. A mean of 64% of the label was found in the apical region (Fig. 7B). Similar ratios were found from immunolabeled human retinas. It is clear from these data, and the data from RPE subcellular fractionation (Fig. 5C), that myosin VIIa is not exclusively on or off melanosomes, or exclusively in the apical or basal region. Nevertheless, these findings are still consistent with the effect of myosin VIIa on melanosome distribution and orientation being a direct consequence of melanosome transport by this motor.

Role of myosin VIIa in the transport of RPE melanosomes

To determine the nature of melanosome transport, we examined the movements of melanosomes in cultured RPE cells from *Myo7a*$^{+/4626SB}$ and *Myo7a*$^{4626SB/4626SB}$ mice by time-lapse microscopy. Static images of the cells by phase-contrast microscopy indicated no apparent difference in the distribution of melanosomes in these cultured cells (Fig. 8A,B). Kymograph analysis of time-lapse microscopy of control RPE showed that melanosomes were either stationary or moved steadily at a slow velocity (mainly in the range of 11–250 nm/second), interrupted by short bursts of faster velocity (>1 μm/second) (Fig. 8C). Melanosomes in *Myo7a*-null cells moved in the same manner, except that the individual bursts of faster movement lasted approximately five times longer (Fig. 8D,E), and more melanosomes were observed undergoing rapid movements (Fig. 8F). Accordingly, fewer melanosomes were observed undergoing slower movements in mutant cells, although it is noteworthy that the slower movements were still present (Fig. 8D,F). This increased motility is clear in movies constructed from the time-lapse images of control and mutant melanosomes (see Fig. S1, in supplementary material). A greater fluctuation in the orientation of melanosomes was also evident in mutant RPE cells. These observations demonstrate that melanosomes do move in RPE cells, that they have movements of different velocities (suggesting the involvement of more than one motor protein – in addition to myosin VIIa), and that the role of myosin VIIa appears to be to constrain the melanosomes from excessive rapid movement.

Discussion

Our results demonstrate the presence of many potential effectors of melanosome motility and localization in the RPE, with a possible role for myosin Va, and a specific requirement for Rab27a and myosin VIIa. The majority (70–80%) of myosin VIIa in the RPE was found to be associated with the membrane of melanosomes, consistent with a role in melanosome transport. Time-lapse microscopy of cultured RPE cells showed that the motility of melanosomes was far greater in the absence of myosin VIIa. Fluorescence microscopy of RPE double-labeled with antibodies and phalloidin shows that the apical distribution of myosin VIIa and myosin Va overlaps with the apical actin filament network. It is this region of overlap from which melanosomes are absent in *Rab27a*- and *Myo7a*-null RPE. Our analysis is consistent with Rab27a and myosin VIIa transporting and capturing melanosomes in this region of the RPE actin network.

Melanosomes in teleost and amphibian RPE undergo quite large movements in response to changes in ambient lighting to effect a light-dark adaptive mechanism (Back et al., 1965; Burnside, 2001). Such changes do not occur in mammalian RPE. Indeed, there have been only a few indications that melanosomes in mammalian RPE move at all. One is implied from the mislocalization of melanosomes in the RPE of *Myo7a*-mutant mice (Liu et al., 1998) (and the present study). Another, more definitively, comes from a detailed analysis of melanosome distribution with respect to time of day in mouse RPE. A small, but significant displacement of melanosomes was detected during the first hours after the lights went on (Futter et al., 2004). Here, by live-cell imaging, we have observed that melanosomes do move in mouse RPE cells (especially in the absence of myosin VIIa).

A role for myosin VIIa in tethering melanosomes compares to its proposed role in inner ear sensory hair cells, where it appears to function in tethering the cell membrane to the actin cytoskeleton of stereocilia (Kros et al., 2002). Moreover, the finding that myosin VIIa is required to constrain the motility and orientation of RPE melanosomes makes the comparison between myosin VIIa in RPE and myosin Va in melanocytes and melanophores quite striking. In melanocytes, the role of myosin Va is to ‘capture’ melanosomes from dendritic microtubules in the periphery of the cell (Wu et al., 1998a). Melanosomes are transported to the periphery by a microtubule motor, at a similar velocity to the rapid movements we measured for RPE melanosomes. In the absence of myosin Va, they are not retained in the periphery and travel back to the cell body (Wu et al., 1998a; Wu et al., 1998b; Wu and Hammer, 2000). In *Xenopus* melanophores, myosin Va has been implicated in promoting the cyclic AMP-sensitive dispersal of melanosomes by acting as a molecular ratchet, increasing the relative contribution of kinesin II-mediated movement over that of cytoplasmic dyenin (Rodionov et al., 1998; Rogers and Gelfand, 1998; Gross et al., 2002).

The movement of RPE melanosomes occurred with at least two distinct velocities, indicating the participation of at least two motor proteins. The measured velocities were of a similar range in control and *Myo7a*-null RPE, indicating that these motor proteins are in addition to myosin VIIa; although slower movements were less evident in the mutant cells, some were still detected. A possible hypothesis is that the more rapid movements (>1 μm/second) are effected by a microtubule motor. Similar to the role of myosin Va in melanocytes (above), myosin VIIa may take delivery of a melanosome from a microtubule motor, and thus normally restrict faster microtubule-based movement. Myosin Va is likely to be involved in the slower movements (11–250 nm/seconds) of melanosomes seen in both control and *Myo7a*-null cells. We found that myosin Va is not required for the correct localization of RPE melanosomes, however, it was enriched in the subcellular fraction containing melanosomes, suggesting a role in melanosome transport, even though it is not essential for the localization of the melanosomes. The movements of melanosomes in teleost RPE in response to lighting changes requires an

intact actin cytoskeleton (King-Smith et al., 1997), and the melanosomes have been shown recently, in elegant motility studies, to contain a plus-end directed myosin(s) (McNeil et al., 2004). Interestingly, however, light-dependent movements of melanosomes still occur in the RPE of mariner zebrafish (Perkins et al., 2004), which lack myosin VIIa (Ernest et al., 2000), indicating that myosin VIIa is not required for these movements. We suggest that myosin Va is a more likely candidate for light-dependent movements.

Myosin VIIa may also participate in the slower movements since relatively fewer melanosomes moved at these velocities in *Myo7a*-null RPE. In vitro, myosin VIIa was found to move along actin filaments at around 200 nm/second (Udovichenko et al., 2002; Inoue and Ikebe, 2003). Of course, the reduction in slower movements could be simply a result of the identification of more melanosomes moving at the fast velocity. However, we have never observed even a single melanosome in an apical process of a *Myo7a*-mutant RPE, suggesting that myosin VIIa is responsible for transporting melanosomes into this region. If it were only responsible for tethering melanosomes, we would expect, at least occasionally, to observe a melanosome in an apical process of a *Myo7a*-mutant RPE. Hence, myosin VIIa appears to move melanosomes in addition to tethering them.

With the finding that Myrip binds both myosin VIIa and Rab27a (El-Amraoui et al., 2002; Fukuda and Kuroda, 2002), together with the mislocalized melanosomes in shaker1 RPE (Liu et al., 1998), it has been suggested that a Rab27a-Myripmyosin VIIa complex might localize RPE melanosomes just as a Rab27a-melanophilin-myosin Va complex is responsible for the peripheral localization of melanosomes in melanocytes (El-Amraoui et al., 2002). Our results support this hypothesis. The finding of the same melanosome phenotype in the RPE of *Rab27a*-mutant mice as in the RPE of *Myo7a*-mutant mice demonstrates the requirement of Rab27a as well as myosin VIIa. This observation has now also been described by another group (Futter et al., 2004). Hence, Rab27a regulation of melanosome localization is conserved between melanocytes and the RPE, yet different myosins are used to tether these organelles in the different cells.

It is not known at present whether Myrip is an obligate member of the localization complex in RPE, as melanophilin is in melanocytes (Provance et al., 2002; Hume et al., 2002). Many different exophilins, which might link myosins to Rab27a on the melanosome membrane, were detected in the RPE – including melanophilin. What seems likely is that the combined tasks of transporting and tethering melanosomes in the RPE may involve many different proteins. Further analysis of melanosome motility is needed to dissect the different functions of the various motors and linkers.

The last point for discussion concerns the requirement of myosin VIIa to maintain vision. As we have discussed previously, it seems unlikely that a mislocalization of RPE melanosomes per se would lead to the photoreceptor degeneration found in Usher 1B patients. A delay in transporting and degrading phagosomes appears to be a more serious RPE defect, caused by the loss of myosin VIIa (Gibbs et al., 2003). However, the present study shows that melanosomes are not only misplaced, but are more highly mobile in the absence of myosin VIIa. Melanosomes ‘on the loose’ may have deleterious consequences for the health of the RPE cells, and thus, in turn, contribute to photoreceptor degeneration.

Supplementary Material

Refer to Web version on PubMed Central for supplementary material.

Acknowledgments

We thank Karen Teofilo and Erin Legacki for technical assistance in the Williams lab, John Hammer for his gifts of myosin Va and Rab27a antibodies, and John Potoky (Alpine Meats) for donating pig eyes. This research was supported by NIH grant EY07042, NIH core grant EY12598, a grant from the Foundation Fighting Blindness, the MRC, Defeating Deafness, the EC (QLG2-CT-1999-00988), and (for the acquisition of the ashen and leaden mice from the JAX Mouse Mutant Resource) NIH grant RR01183.

References

Ahmed ZM, Morell RJ, Riazuddin S, Gropman A, Shaukat S, Ahmad MM, Mohiddin SA, Fananapazir L, Caruso RC, Husnain T, et al. Mutations of MYO6 are associated with recessive deafness, DFNB37. Am. J. Hum. Genet 2003;72:1315–1322. [PubMed: 12687499]

Astuto LM, Weston MD, Carney CA, Hoover DM, Cremers C, Wagenaar M, Moller C, Smith RJH, Pieke-Dahl S, Greenberg J, et al. Genetic heterogeneity of Usher syndrome: analysis of 151 families with Usher type I. Am. J. Hum. Genet 2000;67:1569–1574. [PubMed: 11060213]

Avraham KB, Hasson T, Steel KP, Kingsley DM, Russell LB, Mooseker MS, Copeland NG, Jenkins NA. The mouse Snell's waltzer deafness gene encodes an unconventional myosin required for structural integrity of inner ear hair cells. Nat. Genet 1995;11:369–375. [PubMed: 7493015]

Back I, Donner KO, Reuter T. The screening effect of the pigment epithelium on the retinal rods in the frog. Vision Res 1965;5:101–111. [PubMed: 5862942]

Boeda B, El-Amraoui A, Bahloul A, Goodyear R, Daviet L, Blanchard S, Perfettini I, Fath KR, Shorte S, Reiners J, et al. Myosin VIIa, harmonin and cadherin 23, three Usher I gene products that cooperate to shape the sensory hair cell bundle. EMBO J 2002;21:6689–6699. [PubMed: 12485990]

Burnside B. Light and circadian regulation of retinomotor movement. Prog. Brain Res 2001;131:477–485. [PubMed: 11420964]

Desnos C, Schonn JS, Huet S, Tran VS, El-Amraoui A, Raposo G, Fanget I, Chapuis C, Menasche G, de Saint Basile G, et al. Rab27A and its effector MyRIP link secretory granules to F-actin and control their motion towards release sites. J. Cell Biol 2003;163:559–570. [PubMed: 14610058]

Doucet JP, Trifaro JM. A discontinuous and highly porous sodium dodecyl sulfate-polyacrylamide slab gel system of high resolution. Anal. Biochem 1988;168:265–271. [PubMed: 3364726]

El-Amraoui A, Sahly I, Picaud S, Sahel J, Abitbol M, Petit C. Human Usher 1B/mouse shaker-1: the retinal phenotype discrepancy explained by the presence/absence of myosin VIIA in the photoreceptor cells. Hum. Mol. Genet 1996;5:1171–1178. [PubMed: 8842737]

El-Amraoui A, Schonn JS, Kussel-Andermann P, Blanchard S, Desnos C, Henry JP, Wolfrum U, Darchen F, Petit C. MyRIP, a novel Rab effector, enables myosin VIIa recruitment to retinal melanosomes. EMBO Rep 2002;3:463–470. [PubMed: 11964381]

Ernest S, Rauch GJ, Haffter P, Geisler R, Petit C, Nicolson T. Mariner is defective in myosin VIIA: a zebrafish model for human hereditary deafness. Hum. Mol. Genet 2000;9:2189–2196. [PubMed: 10958658]

Fukuda M, Kuroda TS. Slac2-c (synaptotagmin-like protein homologue lacking C2 domains-c), a novel linker protein that interacts with Rab27, myosin Va/VIIa, and actin. J. Biol. Chem 2002;277:43096–43103. [PubMed: 12221080]

Fukuda M, Kuroda TS, Mikoshiba K. Slac2-a/melanophilin, the missing link between Rab27 and myosin Va: implications of a tripartite protein complex for melanosome transport. J. Biol. Chem 2002;277:12432–12436. [PubMed: 11856727]

Futter CE, Ramalho JS, Jaissle GB, Seeliger MW, Seabra MC. The role of Rab27a in the regulation of melanosome distribution within retinal pigment epithelial cells. Mol. Biol. Cell 2004;15:2264–2275. [PubMed: 14978221]

Gibbs D, Williams DS. Isolation and culture of primary mouse retinal pigmented epithlelial cells. Adv. Exp. Med. Biol 2003;533:347–352. [PubMed: 15180284]

Gibbs D, Kitamoto J, Williams DS. Abnormal phagocytosis by retinal pigmented epithelium that lacks myosin VIIa, the Usher syndrome 1B protein. Proc. Natl. Acad. Sci. USA 2003;100:6481–6486. [PubMed: 12743369]

Gibson F, Walsh J, Mburu P, Varela A, Brown KA, Antonio M, Beisel KW, Steel KP, Brown SDM. A type VII myosin encoded by mouse deafness gene shaker-1. Nature 1995;374:62–64. [PubMed: 7870172]

Gross SP, Tuma MC, Deacon SW, Serpinskaya AS, Reilein AR, Gelfand VI. Interactions and regulation of molecular motors in Xenopus melanophores. J. Cell Biol 2002;156:855–865. [PubMed: 11864991]

Hasson T, Heintzelman MB, Santos-Sacchi J, Corey DP, Mooseker MS. Expression in cochlea and retina of myosin VIIa, the gene product defective in Usher syndrome type 1B. Proc. Natl. Acad. Sci. USA 1995;92:9815–9819. [PubMed: 7568224]

Hasson T, Walsh J, Cable J, Mooseker MS, Brown SD, Steel KP. Effects of shaker-1 mutations on myosin-VIIa protein and mRNA expression. Cell Motil. Cytoskeleton 1997;37:127–138. [PubMed: 9186010]

Hume AN, Collinson LM, Rapak A, Gomes AQ, Hopkins CR, Seabra MC. Rab27a regulates the peripheral distribution of melanosomes in melanocytes. J. Cell Biol 2001;152:795–808. [PubMed: 11266470]

Hume AN, Collinson LM, Hopkins CR, Strom M, Barral DC, Bossi G, Griffiths GM, Seabra MC. The leaden gene product is required with Rab27a to recruit myosin Va to melanosomes in melanocytes. Traffic 2002;3:193–202. [PubMed: 11886590]

Inoue A, Ikebe M. Characterization of the motor activity of mammalian myosin VIIA. J. Biol. Chem 2003;278:5478–5487. [PubMed: 12466270]

King-Smith C, Paz P, Lee CW, Lam W, Burnside B. Bidirectional pigment granule migration in isolated retinal pigment epithelial cells requires actin but not microtubules. Cell Motil. Cytoskeleton 1997;38:229–249. [PubMed: 9384214]

Kros CJ, Marcotti W, van Netten SM, Self TJ, Libby RT, Brown SD, Richardson GP, Steel KP. Reduced climbing and increased slipping adaptation in cochlear hair cells of mice with Myo7a mutations. Nat. Neurosci 2002;5:41–47. [PubMed: 11753415]

Libby RT, Steel KP. Electroretinographic anomalies in mice with mutations in Myo7a, the gene involved in human Usher syndrome type 1B. Invest. Ophthalmol. Vis. Sci 2001;42:770–778. [PubMed: 11222540]

Libby RT, Lillo C, Kitamoto J, Williams DS, Steel KP. Myosin Va is required for normal photoreceptor synaptic activity. J. Cell Sci 2004;117:4509–4515. [PubMed: 15316067]

Lillo C, Kitamoto J, Liu X, Quint E, Steel KP, Williams DS. Mouse models for Usher syndrome 1B. Adv. Exp. Med. Biol 2003;533:143–150. [PubMed: 15180258]

Liu X, Vansant G, Udovichenko IP, Wolfrum U, Williams DS. Myosin VIIa, the product of the Usher 1B syndrome gene, is concentrated in the connecting cilia of photoreceptor cells. Cell Motil. Cytoskeleton 1997;37:240–252. [PubMed: 9227854]

Liu X, Ondek B, Williams DS. Mutant myosin VIIa causes defective melanosome distribution in the RPE of shaker-1 mice. Nat. Genet 1998;19:117–118. [PubMed: 9620764]

Liu X, Udovichenko IP, Brown SDM, Steel KP, Williams DS. Myosin VIIa participates in opsin transport through the photoreceptor cilium. J. Neurosci 1999;19:6267–6274. [PubMed: 10414956]

Matesic LE, Yip R, Reuss AE, Swing DA, O'Sullivan TN, Fletcher CF, Copeland NG, Jenkins NA. Mutations in Mlph, encoding a member of the Rab effector family, cause the melanosome transport defects observed in leaden mice. Proc. Natl. Acad. Sci. USA 2001;98:10238–10243. [PubMed: 11504925]

McNeil EL, Tacelosky D, Basciano P, Biallas B, Williams R, Damiani P, Deacon S, Fox C, Stewart B, Petruzzi N, et al. Actin-dependent motility of melanosomes from fish retinal pigment epithelial (RPE) cells investigated using in vitro motility assays. Cell Motil. Cytoskeleton 2004;58:71–82. [PubMed: 15083529]

Melchionda S, Ahituv N, Bisceglia L, Sobe T, Glaser F, Rabionet R, Arbones ML, Notarangelo A, di Iorio E, Carella M, et al. MYO6, the human homologue of the gene responsible for deafness in Snell's waltzer mice, is mutated in autosomal dominant nonsyndromic hearing loss. Am. J. Hum. Genet 2001;69:635–640. [PubMed: 11468689]

Menasche G, Pastural E, Feldmann J, Certain S, Ersoy F, Dupuis S, Wulffraat N, Bianchi D, Fischer A, le Deist F, et al. Mutations in RAB27A cause Griscelli syndrome associated with haemophagocytic syndrome. Nat. Genet 2000;25:173–176. [PubMed: 10835631]

Mercer JA, Seperack PK, Strobel MC, Copeland NG, Jenkins NA. Novel myosin heavy chain encoded by murine dilute coat colour locus. Nature 1991;349:709–712. [PubMed: 1996138]

Mustapha M, Chouery E, Torchard-Pagnez D, Nouaille S, Khrais A, Sayegh FN, Megarbane A, Loiselet J, Lathrop M, Petit C, et al. A novel locus for Usher syndrome type I, USH1G, maps to chromosome 17q24-25. Hum. Genet 2002;110:348–350. [PubMed: 11941484]

Nagashima K, Torii S, Yi Z, Igarashi M, Okamoto K, Takeuchi T, Izumi T. Melanophilin directly links Rab27a and myosin Va through its distinct coiled-coil regions. FEBS Lett 2002;517:233–238. [PubMed: 12062444]

Pastural E, Barrat FJ, Dufourcq-Lagelouse R, Certain S, Sanal O, Jabado N, Seger R, Griscelli C, Fischer A, de Saint Basile G. Griscelli disease maps to chromosome 15q21 and is associated with mutations in the myosin-Va gene. Nat. Genet 1997;16:289–292. [PubMed: 9207796]

Perkins BD, Matsui JI, Murphy MK, Dowling JE. Histological and physiological abnormalities in myosin VIIA mutant zebrafish. Invest. Ophthalmol. Vis. Sci 2004;45:3591.

Petit C. Usher syndrome: from genetics to pathogenesis. Annu. Rev. Genomics Hum. Genet 2001;2:271–297. [PubMed: 11701652]

Provance DW, James TL, Mercer JA. Melanophilin, the product of the leaden locus, is required for targeting of myosin-Va to melanosomes. Traffic 2002;3:124–132. [PubMed: 11929602]

Rodionov VI, Hope AJ, Svitkina TM, Borisy GG. Functional coordination of microtubule-based and actin-based motility in melanophores. Curr. Biol 1998;8:165–168. [PubMed: 9443917]

Rogers SL, Gelfand VI. Myosin cooperates with microtubule motors during organelle transport in melanophores. Curr. Biol 1998;8:161–164. [PubMed: 9443916]

Schlamp CL, Williams DS. Myosin V in the retina: localization in the rod photoreceptor synapse. Exp. Eye Res 1996;63:613–619. [PubMed: 9068368]

Siemens J, Kazmierczak P, Reynolds A, Sticker M, Littlewood-Evans A, Muller U. The Usher syndrome proteins cadherin 23 and harmonin form a complex by means of PDZ-domain interactions. Proc. Natl. Acad. Sci. USA 2002;99:14946–14951. [PubMed: 12407180]

Strom M, Hume AN, Tarafder AK, Barkagianni E, Seabra MC. A family of Rab27-binding proteins. Melanophilin links Rab27a and myosin Va function in melanosome transport. J. Biol. Chem 2002;277:25423–25430. [PubMed: 11980908]

Udovichenko IP, Gibbs D, Williams DS. Actin-based motor properties of native myosin VIIa. J. Cell Sci 2002;115:445–450. [PubMed: 11839794]

Wang N, Koutz CA, Anderson RE. A method for the isolation of retinal pigment epithelial cells from adult rats. Invest. Ophthalmol. Vis. Sci 1993;34:101–107. [PubMed: 8425817]

Waselle L, Coppola T, Fukuda M, Iezzi M, El-Amraoui A, Petit C, Regazzi R. Involvement of the Rab27 binding protein Slac2c/MyRIP in insulin exocytosis. Mol. Biol. Cell 2003;14:4103–4113. [PubMed: 14517322]

Weil D, Blanchard S, Kaplan J, Guilford P, Gibson F, Walsh J, Mburu P, Varela A, Levilliers J, Weston MD, et al. Defective myosin VIIA gene responsible for Usher syndrome type 1B. Nature 1995;374:60–61. [PubMed: 7870171]

Weil D, El-Amraoui A, Masmoudi S, Mustapha M, Kikkawa Y, Laine S, Delmaghani S, Adato A, Nadifi S, Zina BZ, et al. Usher syndrome type I G (USH1G) is caused by mutations in the gene encoding SANS, a protein that associates with the USH1C protein, harmonin. Hum. Mol. Genet 2003;12:463–471. [PubMed: 12588794]

Wilson SM, Yip R, Swing DA, O'Sullivan TN, Zhang Y, Novak EK, Swank RT, Russell LB, Copeland NG, Jenkins NA. A mutation in Rab27a causes the vesicle transport defects observed in ashen mice. Proc. Natl. Acad. Sci. USA 2000;97:7933–7938. [PubMed: 10859366]

Wu X, Hammer JA III. Making sense of melanosome dynamics in mouse melanocytes. Pigment Cell Res 2000;13:241–247. [PubMed: 10952391]

Wu X, Bowers B, Wei Q, Kocher B, Hammer JA III. Myosin V associates with melanosomes in mouse melanocytes: evidence that myosin V is an organelle motor. J. Cell Sci 1997;110:847–859. [PubMed: 9133672]

Wu X, Bowers B, Rao K, Wei Q, Hammer JA III. Visualization of melanosome dynamics within wild-type and dilute melanocytes suggests a paradigm for myosin V function In vivo. J. Cell Biol 1998a; 143:1899–1918. [PubMed: 9864363]

Wu XF, Kocher B, Wei Q, Hammer JA III. Myosin Va associates with microtubule-rich domains in both interphase and dividing cells. Cell Motil. Cytoskeleton 1998b;40:286–303. [PubMed: 9678671]

Wu X, Rao K, Bowers MB, Copeland NG, Jenkins NA, Hammer JA III. Rab27a enables myosin Va-dependent melanosome capture by recruiting the myosin to the organelle. J. Cell Sci 2001;114:1091–1100. [PubMed: 11228153]

Wu XS, Rao K, Zhang H, Wang F, Sellers JR, Matesic LE, Copeland NG, Jenkins NA, Hammer JA III. Identification of an organelle receptor for myosin-Va. Nat. Cell Biol 2002;4:271–278. [PubMed: 11887186]

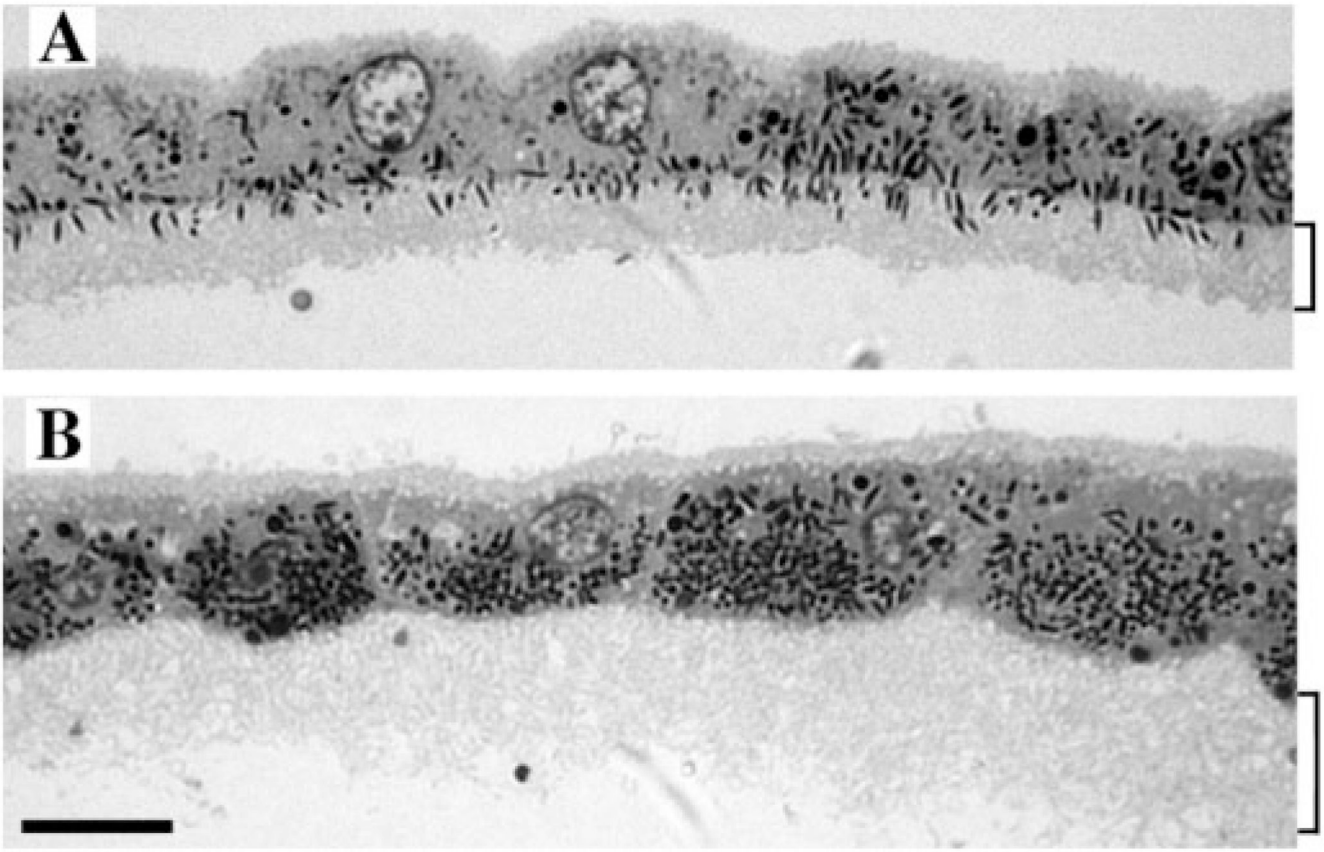

Fig. 1.

Light micrographs of purified sheets of RPE cells from (A) shaker1 control (*Myo7a*$^{+/4626SB}$) and (B) shaker1 mutant (*Myo7a*$^{4626SB/4626SB}$) mouse retinas. Apical processes are evident as lightly stained region below the cell bodies (indicated by square brackets). In the control RPE, melanosomes are present in the apical processes, whereas the apical processes of the mutant RPE are devoid of melanosomes. Bar, 10 μm.

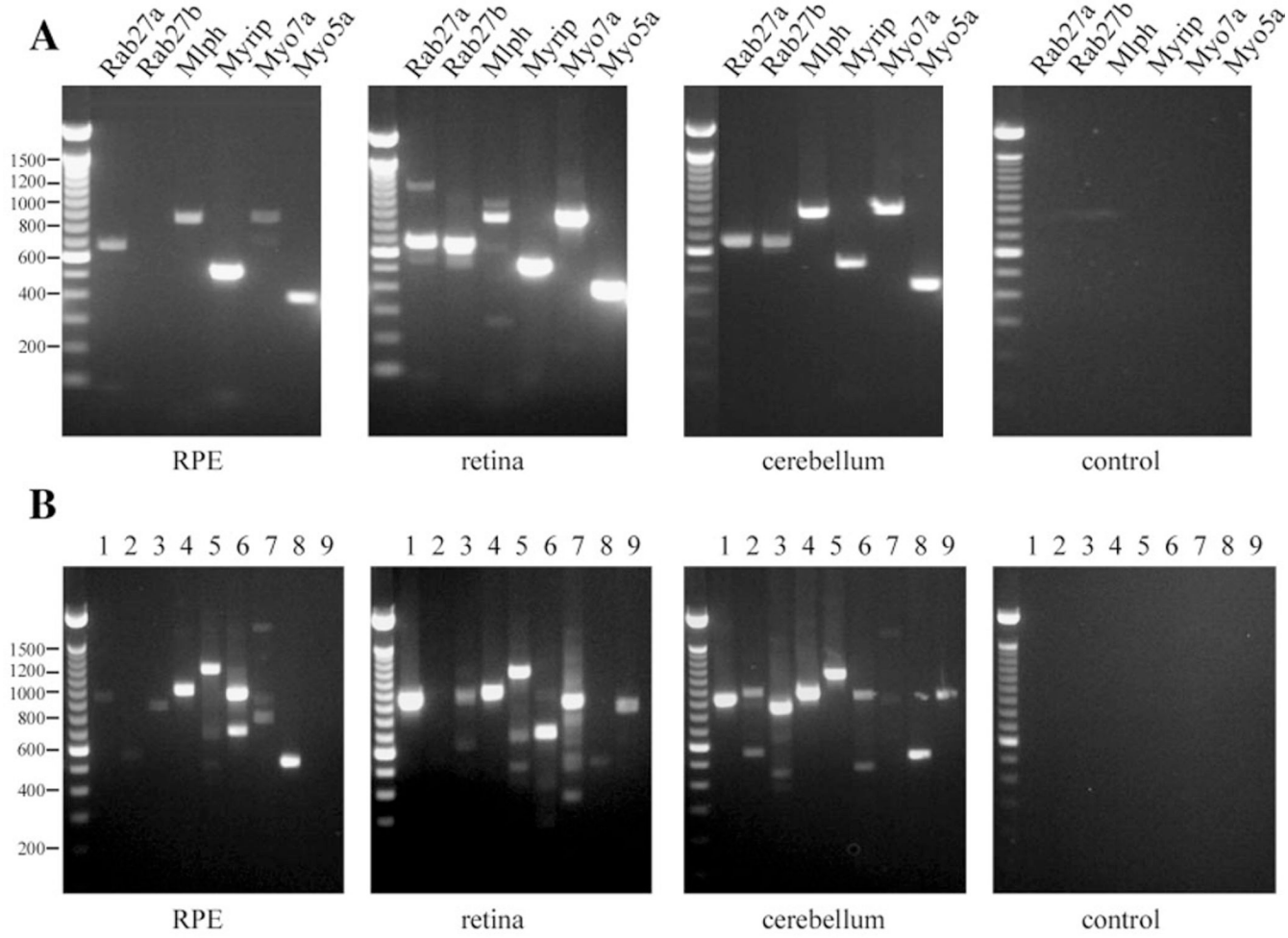

Fig. 2.

RT-PCR of purified mouse RPE cells. (A) Representative RT-PCR of mRNA expression of *Rab27a*, *Rab27b*, Melanophilin (*Mlph*), *Myrip*, *Myo7a* and *Myo5a* in purified mouse RPE cells, retina and cerebellum. Control, PCR reaction without added DNA. The position of DNA size-standards in bp is given at the left. (B) Representative RT-PCR of mRNA expression of different exophilins in purified mouse RPE cells, retina and cerebellum. 1, Exophilin 1-Rabphilin 3a; 2, Exophilin2-Granuphilin-Sytl4; 3, Exophilin3-Melanophilin-Slac2-a; 4, Exophilin4-Sytl2; 5, Exophilin5-Slac2-b, 6, Exophilin6-Sytl3; 7, Exophilin7-Sytl1; 8, Exophilin8-Myrip-Slac2-c; 9, Exophilin9-Sylt5. Control, PCR reaction without added DNA. The position of DNA size-standards in bp is given at the left.

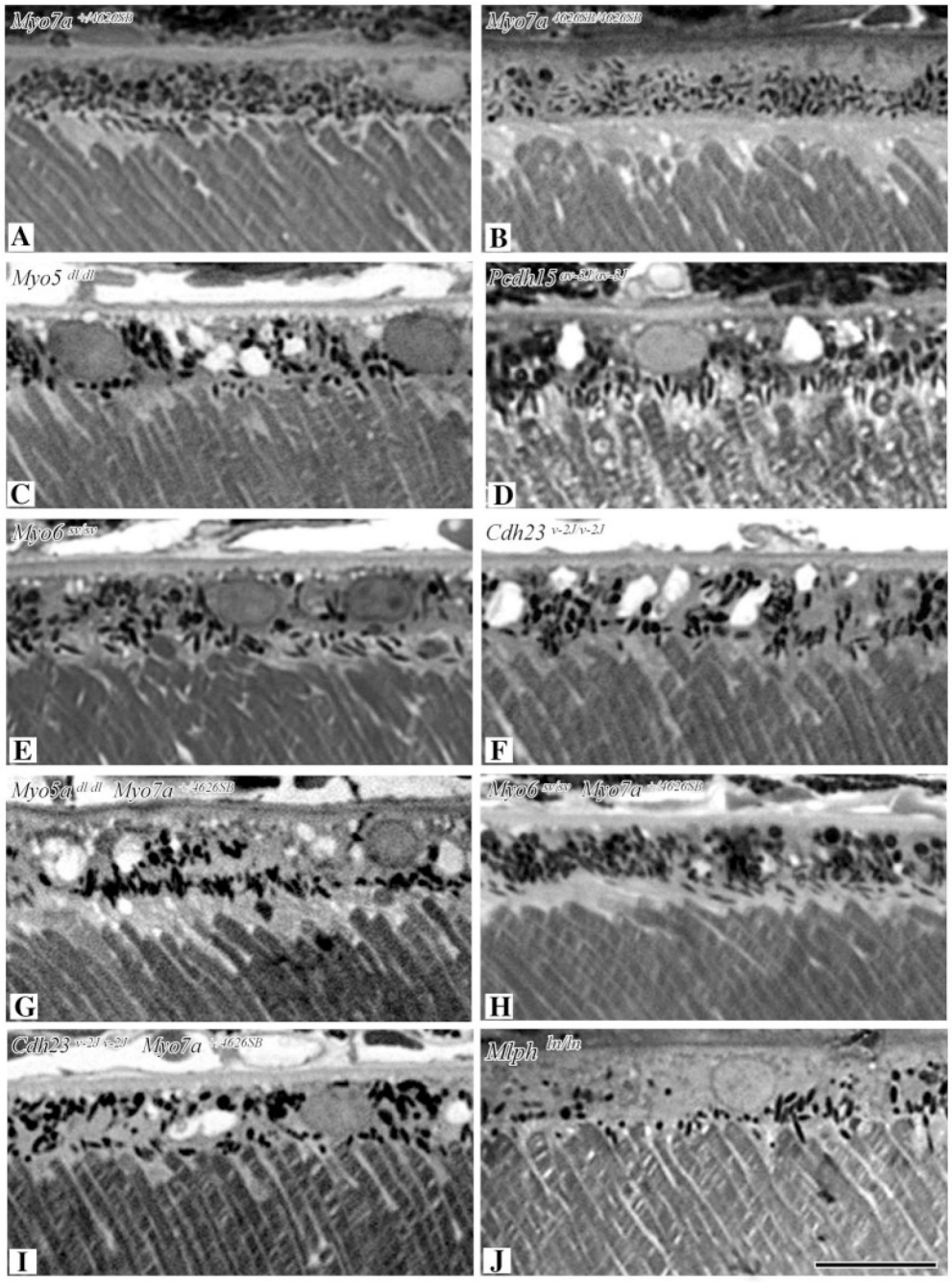

Fig. 3.

Light micrographs of semithin sections of the RPE and outer segments from mice that were (A) shaker1 control (*Myo7a*$^{+/4626SB}$), (B) shaker1 mutant (*Myo7a*$^{4626SB/4626SB}$), (C) dilute lethal (*Myo5a*$^{d\text{-}l/d\text{-}l}$), (D) Ames' waltzer (*Pcdh15*$^{av\text{-}3J/av\text{-}3J}$), (E) Snell's waltzer (*Myo6*$^{sv/sv}$), (F) waltzer (*Cdh23*$^{v\text{-}2J/v\text{-}2J}$), (G) dilute lethal (*Myo5a*$^{d\text{-}l/d\text{-}l}$) plus shaker1 heterozygote (*Myo7a*$^{+/4626SB}$), (H) Snell's waltzer (*Myo6*$^{sv/sv}$) plus shaker1 heterozygote (*Myo7a*$^{+/4626SB}$) and (I) waltzer (*Cdh23*$^{v\text{-}2J/v\text{-}2J}$) plus shaker1 heterozygote (*Myo7a*$^{+/4626SB}$). Genotypes are indicated on each panel. All images are the same magnification (bar, 10 μm).

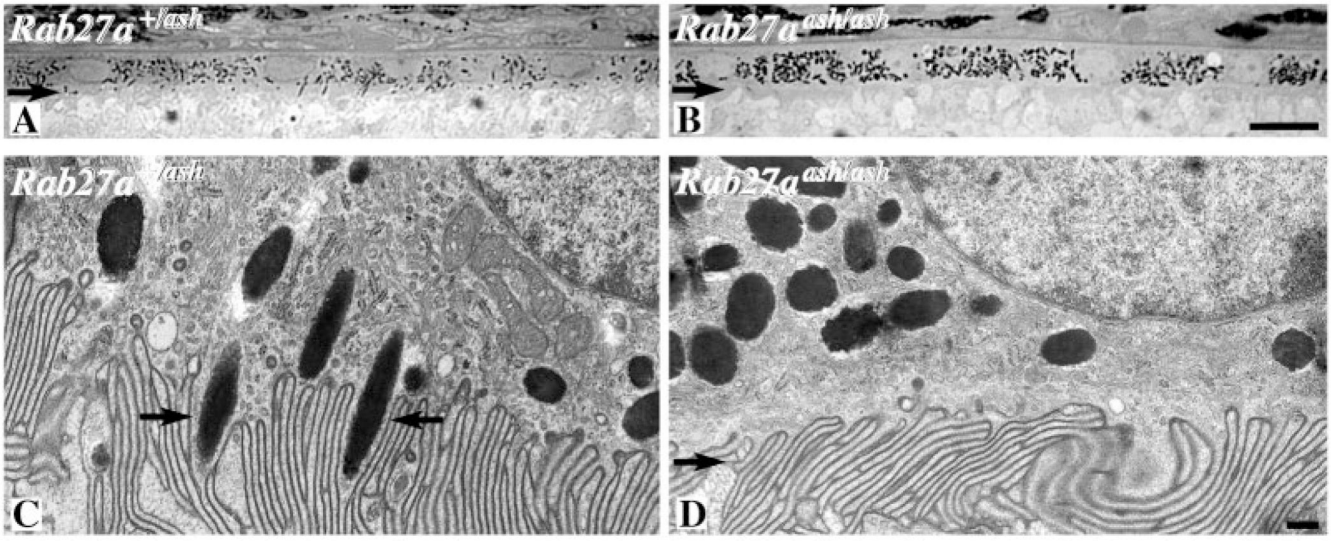

Fig. 4.

Light (A,B) and electron (C,D) micrographs of the RPE from ashen mice. (A,C) Control (*Rab27a*$^{+/ash}$), (B,D) mutant (*Rab27a*$^{ash/ash}$). The mice were on the C3H/HeSn background, which includes the *rd1* mutation. Retinas were obtained from 14-day-old animals. No photoreceptor outer segments are evident owing to the initiation of photoreceptor degeneration, however, at this stage, the RPE remains unaffected by the degeneration. Arrows in A and B indicate the apical region of the RPE, which is completely devoid of melanosomes in the mutant. Arrows in C indicate melanosomes partially contained within the apical processes. Arrow in D indicates the apical processes, with melanosomes some distance away. A is the same magnification as B (bar, 10 μm) and C is the same as D (bar, 100 nm).

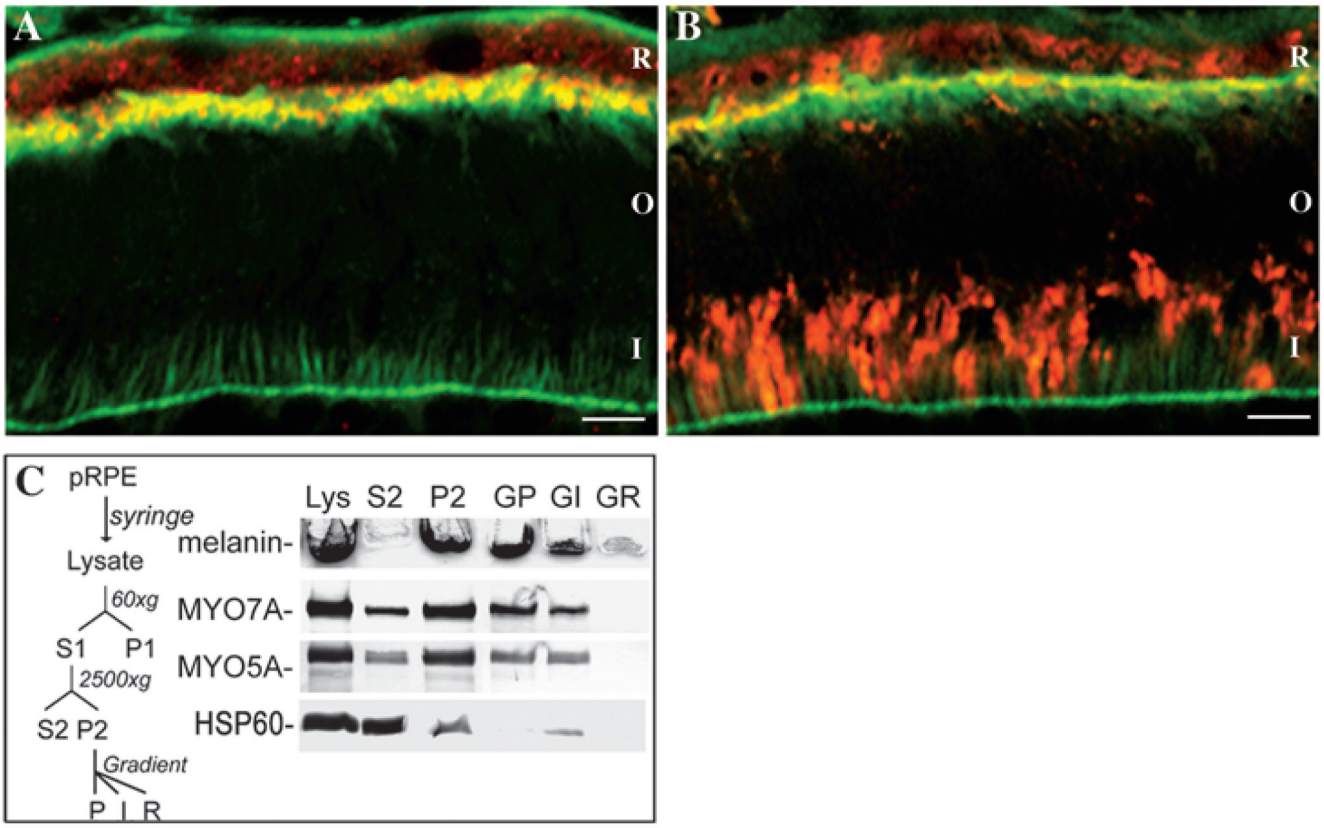

Fig. 5.

Mouse retinal cryosections immunolabeled with antibodies against (A) myosin VIIa or (B) myosin Va (both red), and also labeled with BODIPY-FL-phallacidin (green) to indicate actin filaments. A region of overlap is evident as a yellow band. Myosin Va is also evident in the photoreceptor inner segments. R, RPE; O, photoreceptor outer segments; I, photoreceptor inner segments. Bars, 10 μm. (C) RPE subcellular fractionation and immunoblot analysis. Left: Schematic of the fractionation procedure for purified pig RPE cells. Right: Analysis of RPE fractions. Each fraction was obtained from the same amount of starting material. Top strip: unstained stacking gel showing melanin content of each fraction, as an indication of the distribution of melanosomes. Lower strips: immunoblot labeled with myosin VIIa, myosin Va, and Hsp60 antibodies. All strips are from the same gel. Melanosomes are enriched in P2 and then in GP (and to a lesser extent in GI), following gradient separation. (GP, fraction from bottom of gradient; GI, fraction from interface; R, remainder.) Nuclei, as indicated by Trypan Blue staining were absent from GP. Labeling with Hsp60 antibody (a mitochondrial marker) indicates that mitochondria were depleted from P2 and GP.

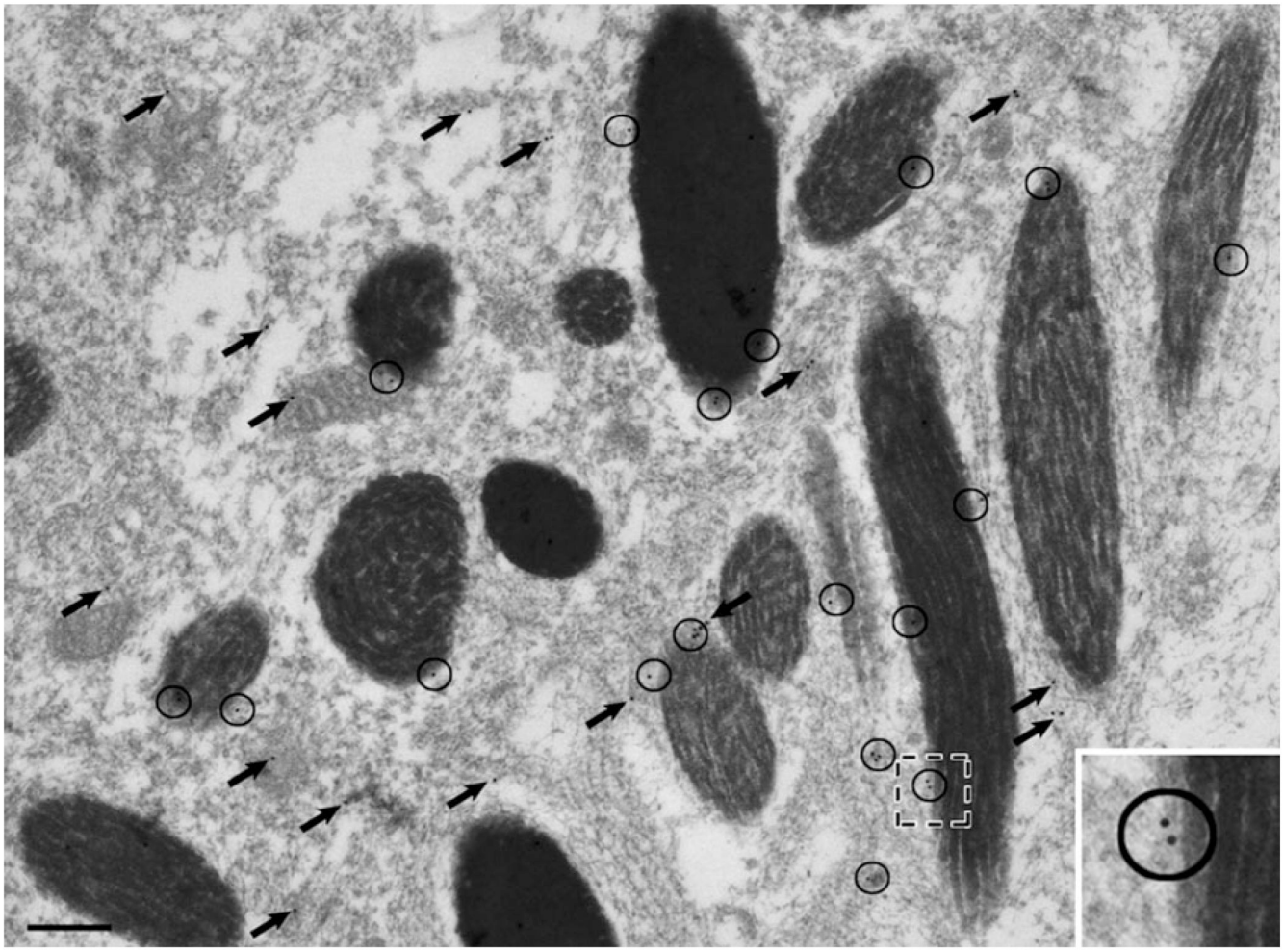

Fig. 6.

Electron micrograph of the RPE from a shaker1 control (*Myo7a*$^{+/4626SB}$) mouse retina immunolabeled with myosin VIIa antibody (10 nm gold particles). The apical region is lower right and the basal region is upper left. In the apical region of the RPE cell, melanosomes are oriented along the axis of the apical processes. Myosin VIIa is present both on the melanosome membrane (circles) and unassociated with the melanosomes, elsewhere in the cytoplasm (arrows). Insert is a magnification of the square in the picture, showing two gold particles associated with the melanosome membrane. Bar, 300 nm.

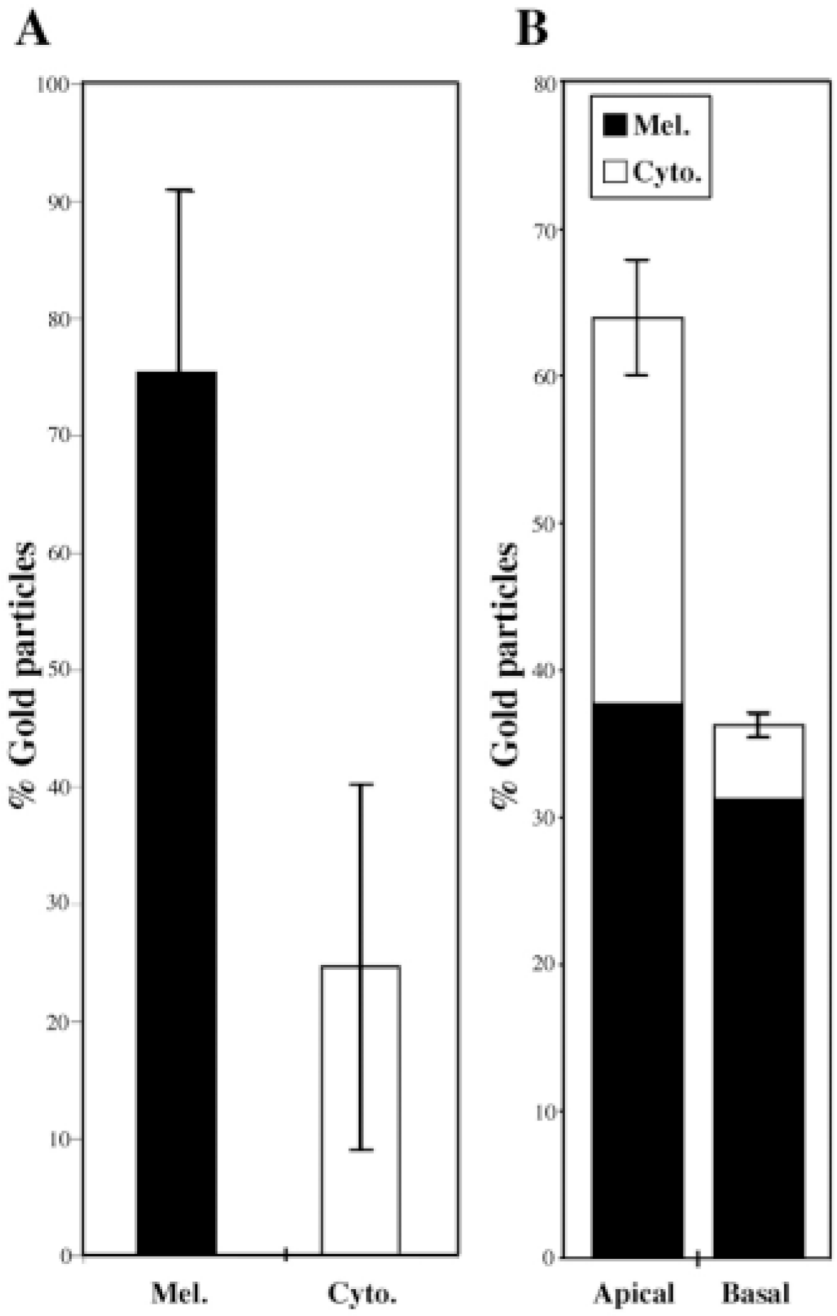

Fig. 7.

(A) Graph showing the percentages of gold particles, representing myosin VIIa labeling, distributed on the melanosome membrane versus those unassociated with the melanosomes but present elsewhere in the RPE cytoplasm. (B) Comparison of the labeling in the regions apical and basal to the adherens junctions of the RPE (relative amount of label on the melanosome membrane is also indicated). Data were obtained from sections with negligible background labeling (there was no labeling on the adjacent ROSs or extracellular space) and negligible labeling on simultaneously-processed, negative control sections.

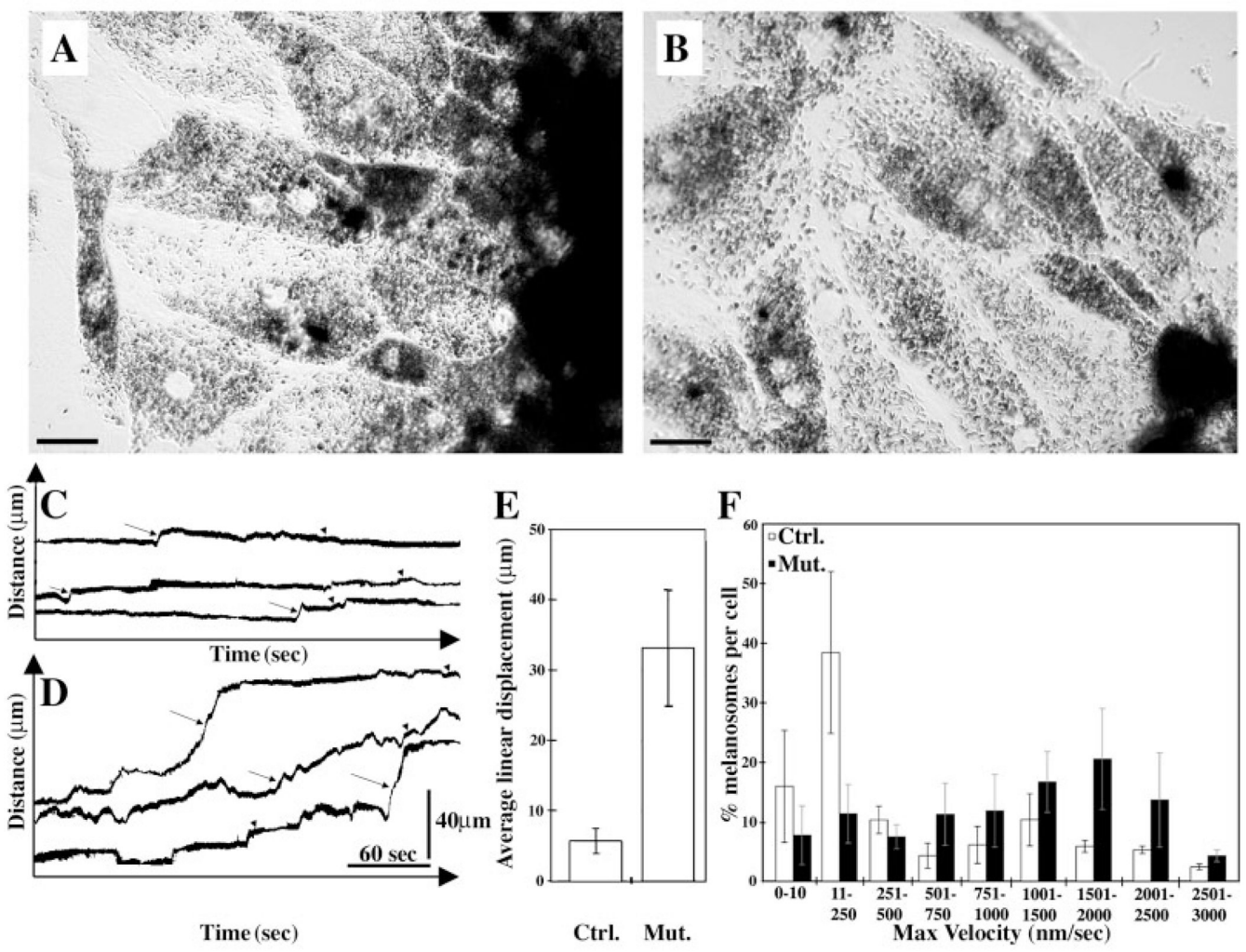

Fig. 8.

Time-lapse microscopy of melanosome movements in cultured RPE cells. Phase-contrast micrographs of RPE cells cultured from (A) shaker1 control (*Myo7a*$^{+/4626SB}$) and (B) shaker1 mutant (*Myo7a*$^{4626SB/4626SB}$) mice. Bars, 20 μm. Representative kymograph traces illustrating the movements of individual melanosomes in control (C) and mutant (D) RPE cells. Arrows indicate bursts of rapid movement, and arrowheads indicate periods of slower movement. (E) Histogram illustrating the mean linear displacement resulting from single continuous rapid movements in control and mutant RPE cells (mean±s.d.). (F) Histogram illustrating the percentage of melanosomes per cell moving at different maximal velocities during 350-second periods in control and mutant RPE cells (mean±s.d.).

Table 1

Primers used for RT-PCR

Gene	Forward primer	Reverse primer	Fragment size (bp)
Exophilin1-Rabphilin 3a	ATGGAAGCAACCACACTGGGTGCC	CTAATCACTGGACACGTGGTT	921
Exophilin2-Granuphilin/Sytl4	ATGAGTGGCTCCTCCATGAGTAC	TTCTGCCCAAGACCCTGGG	974
Exophilin3-Melanophilin/Slac2-a	ATGGTAGACACCTCTGATGAAGA	TTAGGGCTGCTGGGCCATCAC	843
Exophilin4-Sytl2	ATGAGTGGCAGTGTGATGAGCGTT	TCACTTGGAAAGCTTGGCAAT	969
Exophilin5-Slac2-b	ATGAAACACAGATTGGCAGCCAT	TCATAGTTCTGACTCTTTATCCTTT	1155
Exophilin6-Sytl3	ATGAGCACCTGCACAGAGATGGG	TCAGTGCAGGACGAGGGTCAT	948
Exophilin7-Sytl1	ATGGTGCAGGTGCGAGGCTCCGTG	CTATGCCCTGGGGACCAGGTT	900
Exophilin8-Myrip/Slac2-c	GGGACAGACCAAGTGAGACTG	TTAGTACATCACAGCTGACTCCAG	532
Exophilin9-Sylt5	CACATCAGCTACTGCTAC	TCAGAGCCTACATTTCGCCAT	957
MyosinVIIa	CGCGGTAAGGACAGGC	GGTAGCCTCGGAGATATTTGG	829
MyosinVa	ATCAGGTACAATGTCAGTCAA	TCAGACCCGTGCGATGAAGCC	423
Rab27a	ATGTCGGATGGAGATTACGAT	TCAACAGCCACACAACCCCTTC	666
Rab27b	ATGACTGATGGAGACTATGA	CTAGCAGGCACATTTCTT	657